

Supporting Information

Quantification of photoelectrogenerated hydroxyl radical on TiO₂ by surface interrogation scanning electrochemical microscopy

Dodzi Zigah, Joaquín Rodríguez-López, and Allen J. Bard*

Center for Electrochemistry, Department of Chemistry and Biochemistry, University of Texas at Austin, 1 University Station, A5300, Austin, Texas 78712-0165

Abstract

We present additional information about our nanostructured TiO₂ samples and a complete description of the simulation model.

1. Sample characterization

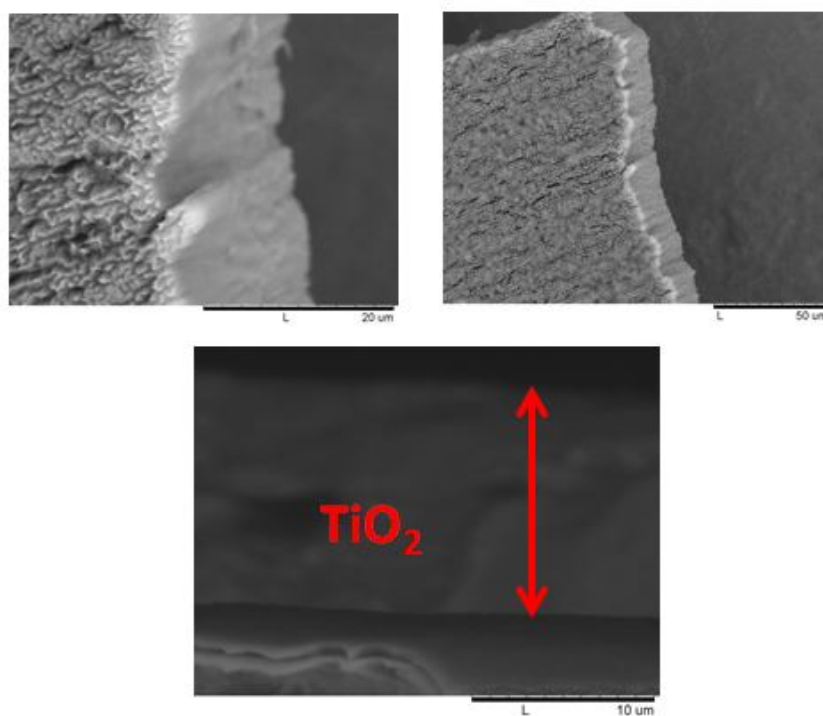


Figure S1. Representative Scanning Electron Microscope images of TiO₂ samples obtained by anodization, as used in this study.

TiO₂ substrates were tested in 1 M HClO₄ to provide a photocurrent of $\sim 0.6 \text{ mA cm}^{-2}$ under a light irradiance of 100 mW cm^{-2} at 1.6 V vs. Ag/AgCl.

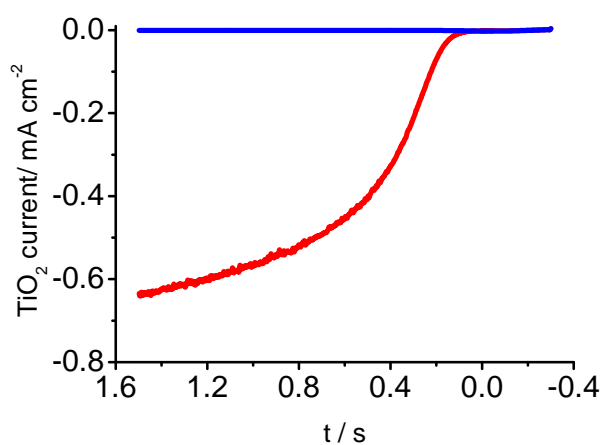


Figure S2: (—) Photocurrent and (—) dark current on TiO₂ in HClO₄ 1 M solution, under xenon lamp irradiation 100 mW cm^{-2} .

2. Simulation Model

Digital simulations of the coupled kinetic and diffusive problem required to describe the SI-SECM response were modeled with COMSOL Multiphysics software v3.2 for a 2D-axial symmetry. The geometry of the simulation space is depicted in Figure S3 and it was adjusted for the experimental conditions of this study, where a tip radius $a = 50 \mu\text{m}$ and $RG = 3$ was used; the substrate was modeled as an active subdomain of radius $b = 150 \mu\text{m}$ and depth $d' = 10 \mu\text{m}$ and is surrounded by an insulating boundary that extends for the length of the remaining bottom of the cell. The interelectrode distance d was adjusted to $27 \mu\text{m}$.

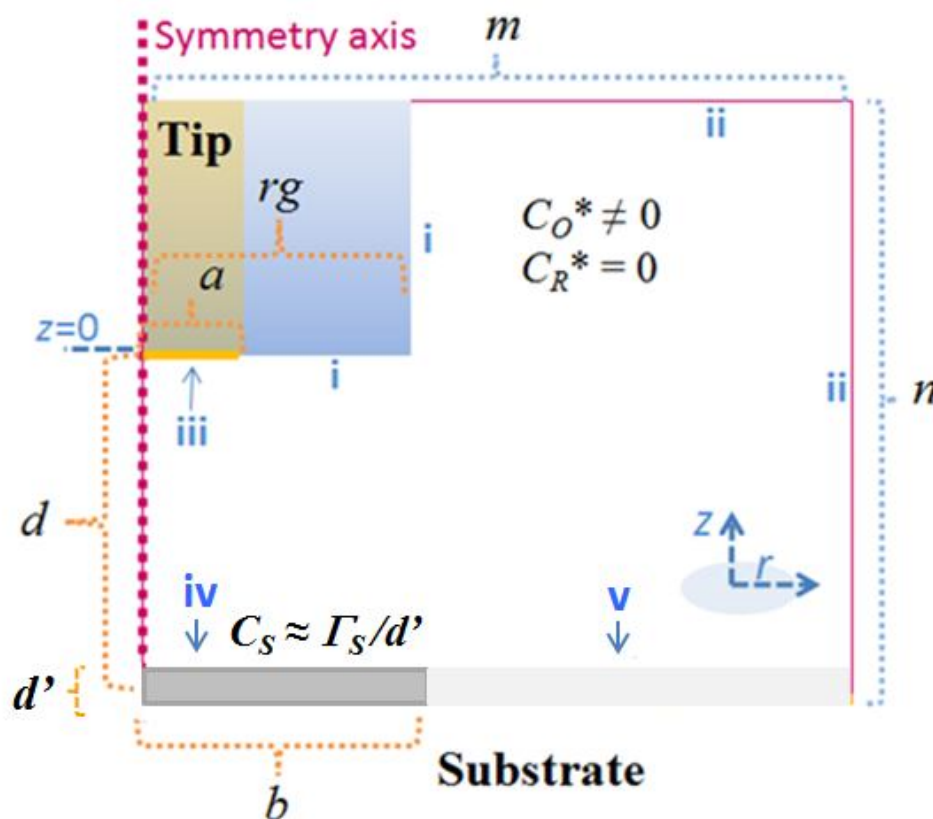


Figure S3. Description of the general SI-SECM simulation space and conditions. All geometries are in axial 2D and described by z and r are shown. Boundary types: i, insulation; ii, bulk

concentration (semi-infinite); iii, flux at the tip; iv, concentration of hydroxyl radical OH at the substrate; v, insulation. In axial 2D, the modeled surface concentration Γ_S was expressed as a pseudo concentration C_S by the conversion factor shown. The length of the cell was $m = n = 20a$. Other quantities as described in the text. Drawing not to scale.

The solution initially contains the oxidized form of the mediator, equal to the bulk value C_{O^*} , and no bulk reduced species, $C_{R^*} = 0$. These bulk values are also used to represent the semi-infinite boundary conditions for type ii boundaries in Figure S3. For the whole domain we considered a diffusion problem in which the reduced species R is being generated at the tip from the initially present oxidized species O . For transient conditions following Fick's second law as required for implementing chronoamperometry we have equations S1 and S2 which apply to the space representing the solution between the two tips (with insulating conditions in the type i boundaries) and extending into bulk of the solution:

$$\frac{\partial C_O}{\partial t} = D_O \nabla^2 C_O \quad (\text{S1})$$

$$\frac{\partial C_R}{\partial t} = D_R \nabla^2 C_R \quad (\text{S2})$$

where C_O and C_R are the concentrations of oxidized and reduced species, respectively and are functions of r , z and time, t . D_O and D_R are the diffusion coefficients of these species and assumed to be $7.2 \times 10^{-10} \text{ m}^2 \text{ s}^{-1}$ corresponding to $\text{IrCl}_6^{2-/3-}$. The tip boundary condition was programmed using the Butler-Volmer formalism to represent the flux towards it. The tip programming was set to be activated at the end of the delay time τ_2 by stepping into a potential

where diffusion limited conditions for the generation of the reduced species apply, while during τ_1 it is set to a potential where the reduced species is not produced at a significant rate. This was accomplished by setting a step function that controlled the value of the potential in a way that during τ_1 its value was 0.15 V and that after τ_2 its value was -0.15 V, in both cases versus a standard potential $E^0 = 0$ which recreates the experimental conditions. At the tip boundary (type iii), $z = 0$, $0 < r < a$, we write the inward flux condition, equations S3 and S4, and the condition for the stepped potential, equation S5:

$$-D_o \nabla C_o = -k^o e^{-\alpha f(E-E^0)} C_o(0,r) + k^o e^{(1-\alpha)f(E-E^0)} C_R(0,r) \quad (\text{S3})$$

$$-D_R \nabla C_R = k^o e^{-\alpha f(E-E^0)} C_o(0,r) - k^o e^{(1-\alpha)f(E-E^0)} C_R(0,r) \quad (\text{S4})$$

$$E = \delta(t); \delta(t) = 0.15 \text{ V } (t < \tau_2); \delta(t) = -0.15 \text{ V } (t > \tau_2) \quad (\text{S5})$$

where k^o is the heterogeneous rate constant set to 10 cm/s, α the transfer coefficient (set to 0.5) and f which is equal to 38.94 V^{-1} at 298 K. The total simulated time was equal to $40 \text{ s} + \tau_2$. The current read at the tip was obtained by integrating the normal diffusive flux of the oxidized species O at its surface and multiplying times a geometric argument as shown in Equation S6:

$$i_T = \int_{r=0}^{r=a} 2\pi n F D_o r \frac{\partial C_o(r,0)}{\partial z} dr \quad (\text{S6})$$

We assumed that the number of electrons transferred was $n = 1$; F is Faraday's constant, 96,485 C/mol. The tip current under transient feedback conditions will be a function of the regeneration of O at the substrate, which will be dependent on the rate of reaction of R with the adsorbed hydroxyl radical $\cdot\text{OH}_{(\text{ads})}$. This reaction takes place only in the volume element where the adsorbed species is present, iv in Figure S3., Equation S7 was implemented to simulate the interrogation process, represented by its surface coverage C_S at the substrate as well as side chemical processes denoted r_{chem} . This last term took the shape of Equation S8 for the competing second order decay of hydroxyl radical and that of Equation S9 in the experiments in the presence of methanol, where k'_{MeOH} is a pseudo-first order rate constant.

$$\frac{\partial C_S}{\partial \tau} = -k_{SI} C_R C_S - r_{\text{chem}} \quad (\text{S7})$$

$$r_{\text{chem}} = 2k_{OH} (C_S)^2 \quad (\text{S8})$$

$$r_{\text{chem}} = 2k_{OH} (C_S)^2 + k'_{\text{MeOH}} C_S \quad (\text{S9})$$

The figure S4 represents the experimental and the theoretical curve (same on figure 9) using a logarithmic scale. With this scale a little “bump” characteristic of the reaction between the hydroxide radical and the mediator can be observed at $t \approx 1$ s. Before 1s we see a small difference between the experimental curve and the theoretical curve. This difference can be explain by the reaction of small oxide present on the microelectrode surface, and a small capacitive current due to the double layer charging.

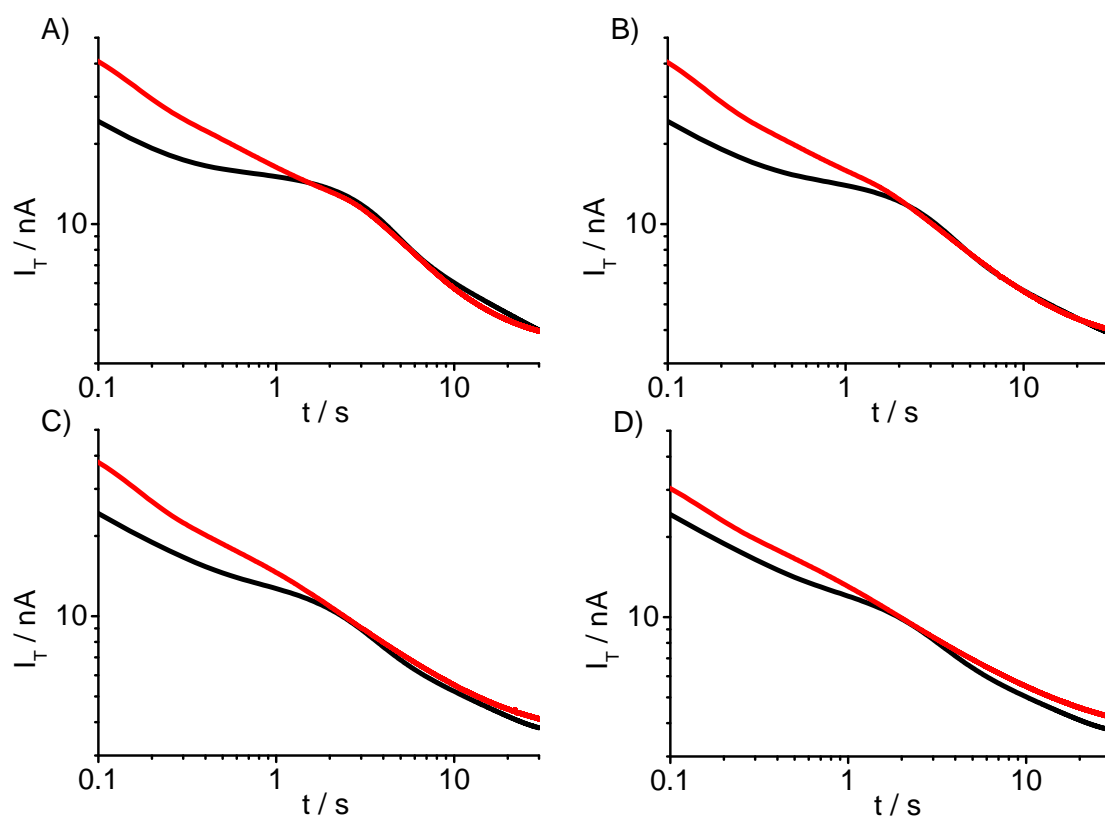


Figure S4 : Surface interrogation of $\cdot\text{OH}_{(\text{ads})}$ at different delay times, τ_2 : (—)

experimental curve; (—) theoretical curve. TiO_2 microelectrode with radius $b = 150$

μm , interrogator: gold UME $a = 50$ μm ; solution 0.1 M HClO_4 with 0.5 mM $\text{K}_2\text{Ir}^{(\text{IV})}\text{Cl}_6$;

$d_{\text{tip-sub}} = 30$ μm , illumination time τ_1 for $\cdot\text{OH}_{(\text{ads})}$ interrogation was 3 s and $E_s = 0.5$ V

vs. Ag/AgCl with A) $\tau_2 = 0.5$ s, B) $\tau_2 = 5$ s, C) $\tau_2 = 15$ s, D) $\tau_2 = 30$ s.